sustainability

MDPI

Article

Comparison of Different Solutions for a Seismic and Energy Retrofit of an Auditorium

Alessandra De Angelis [1,*], Francesco Tariello [2], Rosa Francesca De Masi [1] and Maria Rosaria Pecce [3]

[1] Department of Engineering, University of Sannio, 82100 Benevento, Italy; rfdemasi@unisannio.it
[2] Department of Agricultural, Environmental and Food Sciences, University of Molise, 86100 Campobasso, Italy; francesco.tariello@unimol.it
[3] Department of Structures for Engineering and Architecture, University of Naples Federico II, 80125 Naples, Italy; pecce@unina.it
* Correspondence: adeangelis@unisannio.it

Abstract: The increasing attention paid to climate change has boosted scientific research in the matter of energy refurbishment of existing public buildings. However, the design of the intervention must be integrated with structural upgrading when the constructions are located in seismic zones. Indeed, in Italy, as in other seismically active countries, the structural damage, observed after earthquakes, underlines the increase in economic losses for buildings retrofitted only for energy saving. In this framework, the paper introduces an integrated approach for selecting retrofit actions aimed at improving both the seismic and energy performance, starting from a detailed in situ analysis with which dynamic energy and structural simulation models are constructed. The case study is an auditorium erected in 1982 with a reinforced concrete structure inside a masonry ring wall of an ancient building. A step-by-step analysis of each component role in the structural and energy performance of the building is proposed. The results indicate that the proposed approach can help to determine the best technical solution, and the integrated design leads to saving 10% of the cost of the works.

Keywords: assessment of existing building; structural behavior; energy performance; multidisciplinary approach; cost-benefit

check for updates

Citation: De Angelis, A.; Tariello, F.; De Masi, R.F.; Pecce, M.R. Comparison of Different Solutions for a Seismic and Energy Retrofit of an Auditorium. *Sustainability* **2021**, *13*, 8761. https://doi.org/10.3390/su13168761

Academic Editor: Steve Kardinal Jusuf

Received: 29 June 2021
Accepted: 3 August 2021
Published: 5 August 2021

Publisher's Note: MDPI stays neutral with regard to jurisdictional claims in published maps and institutional affiliations.

Copyright: © 2021 by the authors. Licensee MDPI, Basel, Switzerland. This article is an open access article distributed under the terms and conditions of the Creative Commons Attribution (CC BY) license (https://creativecommons.org/licenses/by/4.0/).

1. Introduction

In recent years, much attention has been paid to the refurbishment of existing buildings in order to comply with European Directives in the matter of energy efficiency. The most recent document, Directive 2018/844 [1], indicates that each Member State shall establish a long-term renovation strategy to support the renovation of the national stock of residential and non-residential buildings, both public and private, into a highly energy-efficient and decarbonized building stock by 2050.

As a result, the scientific community has focused on the methodology for the building refurbishment [2,3], also taking into account economic and environmental indicators [4]. For the building refurbishment in Italy, the reference is the Ministerial Decree of 26 June 2015 [5] on the "Application of the energy performance calculation methods and establishment of buildings' prescriptions and minimum requirements". In compliance with this Decree, during the design phase, many parameters must be checked, ranging from the features of single components to the energy performance of the whole building. In more detail, during the refurbishment, the insulation level must be improved with reduction in thermal transmittance. The threshold values change with the Italian climatic zones: for walls, the limit values vary from 0.40 W/m^{2}K (hot climate) to 0.26 W/m^{2}K (cold climate); for basements, from 0.42 W/m^2 K to 0.28 W/m^2 K; for floors, from 0.32 W/m^2 K to 0.22 W/m^2 K and 0.80 W/m^2 K for partitions. Moreover, in terms of thermal inertia of the

opaque envelope, on all sides except north, north-east and north-west, Y_{IE} must be lower than 0.10 W/(m^2 K); for the floors, it must be lower than 0.18 W/(m^2 K).

Nevertheless, these interventions are usually carried out on buildings without verification of the structural performance, even in the case of buildings designed according to old standards and codes and that are therefore deficient in terms of seismic resilience. Instead, recent seismic events outlined the fact that the failure of the envelope components is responsible for high economic losses resulting from post-earthquake reparation interventions [6]. Furthermore, in Italy in 2003, it was established that seismic analysis of strategic buildings is mandatory [7] according to the standards [8,9]. Therefore, interventions aimed at improving only energy efficiency without addressing safety are bound to failure [10], since the European building stock is deficient in both aspects (energy efficiency and seismic safety).

Despite the necessity of both refurbishments, structural and energy interventions usually follow their own paths and join only towards the end of the process. Therefore, only in recent years have some researchers focused on combined seismic and energy retrofitting approaches to the problem of singular components such as masonry walls [11,12] or reinforced concrete (RC) building envelopes [13]. Few examples of an integrated methodology have been developed in recent years; it can also be remarked that simultaneous investigations and modeling can optimize the costs for the design of the energetic and structural improvements [14]. For example, in [15], a methodology for characterizing seismic and energetic vulnerability of residential RC buildings by means of the fragility curves has been introduced, while Menna et al. [16] proposed an integrated retrofit design methodology for the structural and energy improvement of existing school buildings. Moreover, multidisciplinary approaches for maximizing the benefit of integrated retrofit strategies have been proposed in [17,18].

The available studies indicate that the topic of the combined evaluation of structural and energy performance still needs to be investigated to optimize the whole performance and to reduce the costs, with, at the same time, improvement in safety and comfort. Using a case study, in this paper, a methodology to assess the energy and structural behavior of the existing buildings is proposed using the results to design its upgrade for both aspects.

By means of a combined approach with in situ tests and numerical analyses, the structural and energy deficiencies are evaluated and the role of each building component that affects the performance is identified. Then, the refurbishment scenarios are analyzed by considering the weight of each intervention and by studying the retrofit actions. Finally, a discussion of the cost-benefit analysis of the adopted integrated approach is proposed.

2. The Case Study

A good requalification process starts with the analysis of the original design in order to achieve good knowledge of the structural and architectural details. The selected case study is characterized by both structural and energy deficiencies, and it is particularly suitable for the proposed aim because it is made with a mixed structure (reinforced concrete and masonry) and with boundary conditions that highlight different problems of the building envelope, thus allowing for the development of both global and local interventions.

2.1. Description

The case study is the auditorium of the Astronomical Observatory of Capodimonte, one of the twelve Italian observatories of the National Institute of Astrophysics (INAF), the main Italian company for astronomical and astrophysical research from land and space.

The whole complex (Figure 1a) is located on the top of the Miradoris hill in the city of Naples, and it comprises three separate structures as shown in Figure 1b: the monumental historical building built in 1819 and thoroughly analyzed by De Angelis et al. [19]; the auditorium built in 1982, although the equipment of the internal room dates back to 1990; and the library built in 1990.

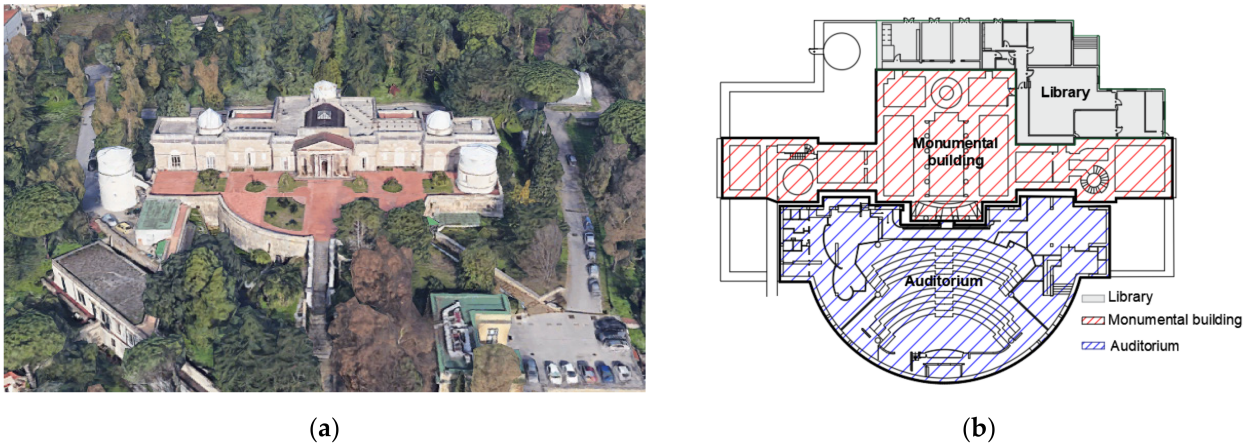

(**a**) (**b**)

Figure 1. (**a**) General overview; (**b**) layout of the three separate structures.

The building is located inside the old tuff boundary wall built in 1819. Its roof provides access to the terrace of the monumental building. The central part of the building is occupied by the multifunctional room with a capacity of about 270 seats, while the lateral wings of the building are dedicated to the museum.

The bearing structure of the building is composed of reinforced concrete (RC) mixed frame-walls and the tuff masonry boundary wall. Inside the building, there are both hollow clay brick (8 cm thick) and plasterboard partitions, as shown in Figure 2. The detected geometrical characteristics are also needed for defining reliable numerical models of the building, aimed at simulating its energy performance. The net conditioned building area is equal to 857 m^2. The "surface-to-volume ratio" (S/V) is equal to 0.65 m^{-1}, and thus its shape factor indicates high heat gain/loss.

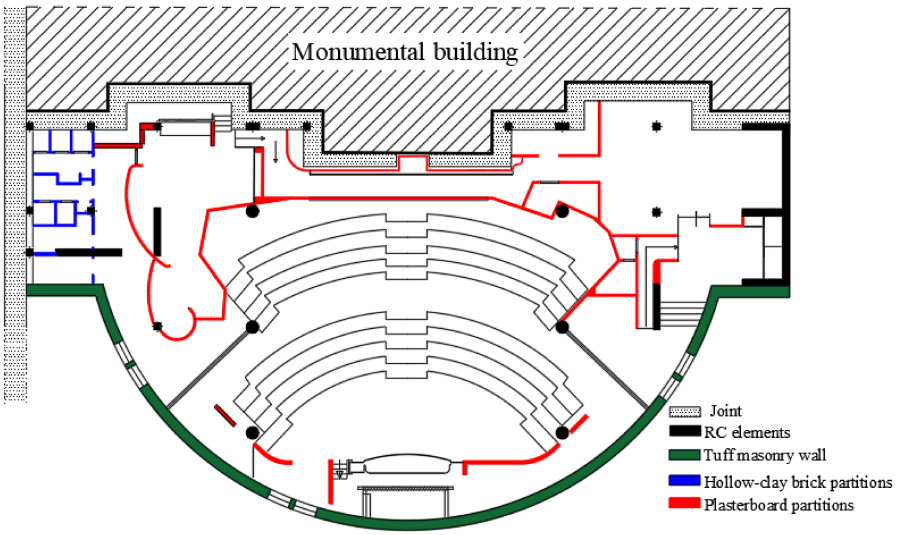

Figure 2. Architectural layout.

It is worth underlining that there are two cavities: the first one separates the building from the tuff walls of the monumental building in the back, while the second one is located adjacent to the left wing of the building to allow a connection with another building in the Astronomical Observatory complex.

The building has suspended ceilings, but it is possible to identify three types of floors: A: RC floor slab with lightening bricks; B: steel-concrete composite floor (steel profiles with RC slab); C: RC floor slab. The main features of the floors are reported in Tables 1–3.

Table 1. Main features of floor A—RC slab with lightening bricks.

Layer	Thickness (m)	Specific Weight (kN/m^3)	Conductivity (W/m K)	Specific Heat (J/kg K)
brick	0.28	8		
RC joist	0.28	25	R = 0.35 m^2 K/W	1000
RC slab	0.04	25		
screed	0.02	19	0.58	1000
filling	0.5	18	1.41	1000
tiled floor	0.02	20	1.30	840

Table 2. Main features of floor B—steel-concrete composite floor.

Layer	Thickness (m)	Specific Weight (kN/m^3)	Conductivity (W/m K)	Specific Heat (J/kg K)
corrugated sheet	0.0006		155	460
RC slab	0.18	25	1.91	1000
screed	0.02	19	0.58	100
filling	0.5	18	1.41	1000
tiled floor	0.02	20	1.30	840

Table 3. Main features of floor C—RC slab.

Layer	Thickness (m)	Specific Weight (kN/m^3)	Conductivity (W/m K)	Specific Heat (J/kg K)
RC slab	0.20	25	1.91	1000
screed	0.02	19	0.58	1000
filling	0.5	18	1.41	1000
tiled floor	0.02	20	1.30	840

In situ surveys to assess structural performance were also useful for characterizing the thermophysical properties of the materials; knowledge of the thicknesses and type of each envelope component is relevant for the resolution of the heat transfer phenomena throughout the building. In more detail, in the following tables, thermal conductivity (λ) and specific heat (c_p) are reported according to the standard UNI 10351 [20]. For non-homogenous floors, such as the concrete-brick one, the equivalent thermal resistance (R) has been considered. The proposed standard suggests the most reliable procedure for both research and design when measurements are not available. However, the proposed values have been verified by means of comparison with the materials used for buildings of the same construction period.

In all three cases, it is also necessary to take into account a layer of plasterboard (2.0 cm, $\lambda = -0.21$ W/m K) at the floor intrados under the false ceiling (90 cm) in which the channels and air handling units are located. Indeed, presently, the building has an all-air system for the needs of heating, cooling, and ventilation. These are fueled during the heating season by means of the hot thermal-vector fluid produced by gas boilers and by means of cold water produced by an electric heat pump during the summer. During the activation days, the building is heated to 20 °C and cooled to 26 °C with a relative humidity of 50%. The air-conditioning system is turned on half an hour before the building is occupied and switched off when the building is empty. It hosts educational activities for students or shows for tourists. The occupancy schedule for the days from Monday to Saturday and for Sunday is shown in Figure 3. A maximum of 200 people is considered.

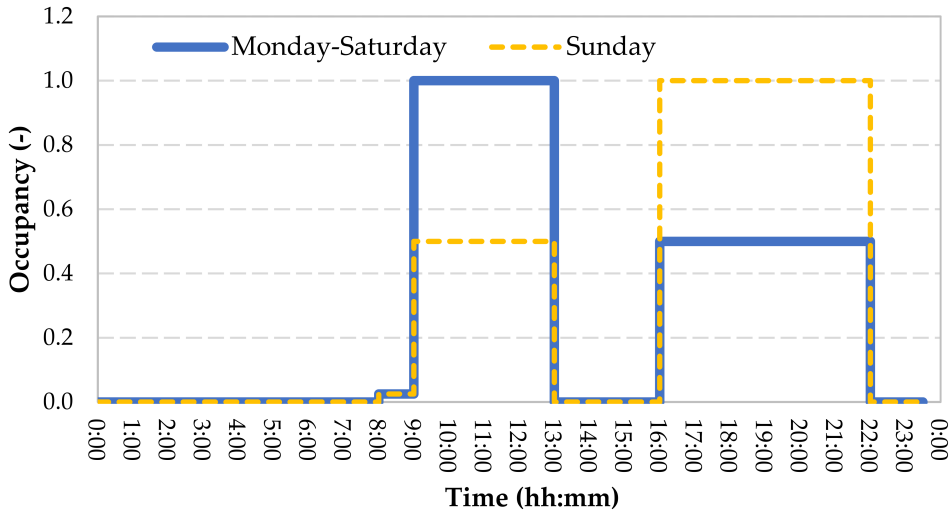

Figure 3. Occupancy schedule.

2.2. Climatic Zone and Seismic Pericolosity

The city of Naples is inside Italian Climatic Zone "C", characterized by 1316 heating degree days (baseline 20 °C), with the duration of the heating period being established from 15 November to 31 March, according to Italian law. The city is located in the southern part of the Italian peninsula (lat. N 40°50′, long. E 14°18′), with a typical Mediterranean climate characterized by warm summers and winters that are not cold. The city is classified Csa according to the Köppen–Geiger standard [21]. Figure 4 shows the maximum, minimum, and average monthly values of air temperature [22], as well as the average precipitation. The average value of the annual temperature is 16.5 °C, with almost 1080 mm of rain. The month characterized by the highest rainfall is November, while July is the most arid. The monthly average humidity varies from 70% (July and August) to 77% (November, December, January).

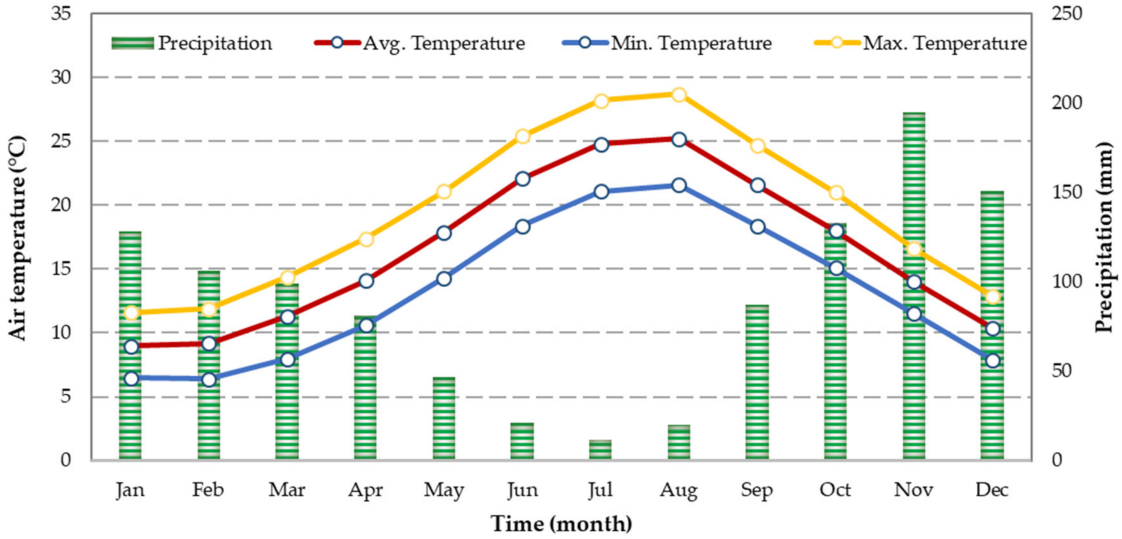

Figure 4. Trend of air temperature (maximum, minimum, and average) and precipitation.

From a structural point of view, Naples is located in a zone with medium seismic risk. The seismic action, useful for the structural simulation at the ultimate limit state, will be evaluated by the elastic response spectrum provided by the Italian Building Code for a returned period TR equal to 712 years and soil type B. The returned period depends on the importance coefficient Cu equal to 1.5 corresponding to a building class III since

high occupancy is assumed for the building. The well-known parameters used for the determination of the elastic acceleration spectrum are reported in Table 4 for the horizontal and vertical spectra at the life-safety limit state (SLV).

Table 4. Parameters of the elastic spectrum.

Spectrum	ag (m/s^2)	F_0 (-)	T*c (s)	S_S (-)	S_T (-)	TB (s)	TC (s)	TD (s)
Horizontal	1.88	2.41	0.34	1.20	1.20	0.15	0.46	2.37
Vertical	1.88	2.41	0.34	1.00	1.20	0.05	0.15	1.00

3. Assessment of the Structural Safety of the Auditorium As-Built

In order to identify the building deficiencies and the requalification needs, in situ visual inspection and material tests were carried out to develop a numerical model for the structure. Then, the developed model was adopted to carry out a linear static analysis for gravity loads at the ultimate limit state (ULS), a modal analysis, and a "linear dynamic analysis with response spectrum" for the seismic assessment.

3.1. Structural Configuration and In Situ Tests

The case study presents a hemicycle shape, and it has a reinforced concrete mixed frame-walls structure (Figure 5). The frames of the lateral wings of the building are characterized by deep beams (cross dimensions = 0.40 × 0.90 m^2), flat beams (section dimensions = 0.40 × 0.32 m^2), and square columns (0.40 × 0.4 m^2); the floors are made of cast-in-place RC and hollow clay bricks as lightening for a total height of 32 cm.

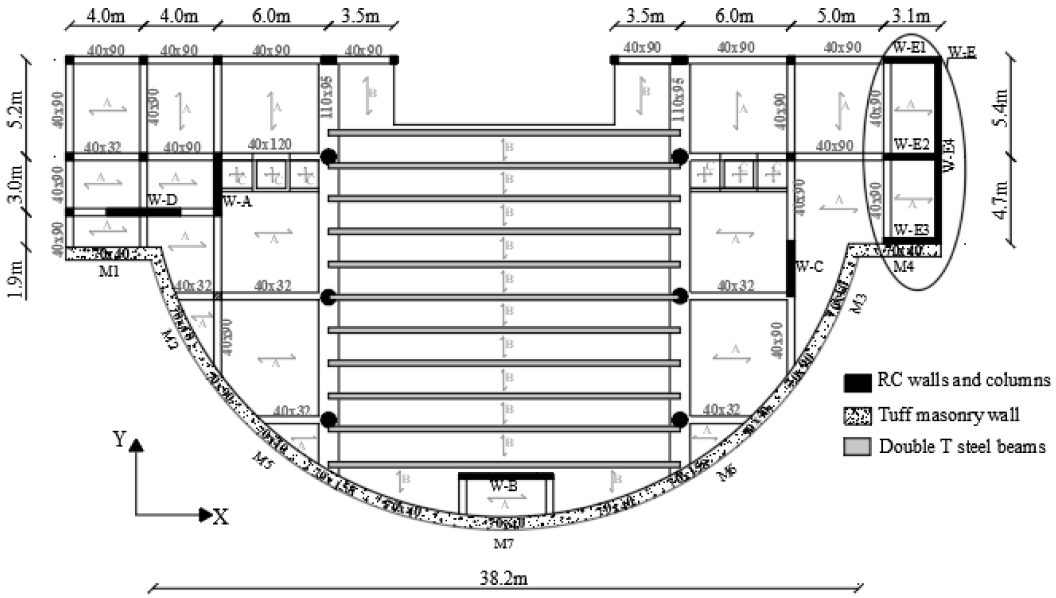

Figure 5. Structural layout of the case study building.

The central part has two side frames consisting of a beam (section dimensions = 1.10 × 0.90 m^2) supported by circular columns (diameter Φ 80 cm) and a steel-concrete composite floor.

Only a few documents of the original design were found; therefore, a wide on-site survey campaign was carried out to define the geometric dimensions of the structural elements. The mechanical characterization of concrete and reinforcement steel was carried out, obtaining an average cylindrical compressive strength of 20.4 MPa and yield strength of 414 MPa, respectively. A double flat jack was carried out for the characterization of the tuff masonry, which gave a compressive strength of 1.25 MPa and a Young modulus of

349 MPa. The detailing of the steel reinforcement was designed by a simulation according to the provisions existing in Italy before 1980, and some checks were carried out in situ.

It is worth underlining that a level of knowledge, according to the current Italian Code [8], equal to LC1 (FC = 1.35) and LC2 (FC = 1.2), was reached for the reinforced concrete part of the building and the tuff masonry boundary wall, respectively.

3.2. Numerical Analysis

The structural analyses were performed using the finite element code SAP2000 [23]. The model shown in Figure 6 was developed according to geometric survey and the characterization of the materials.

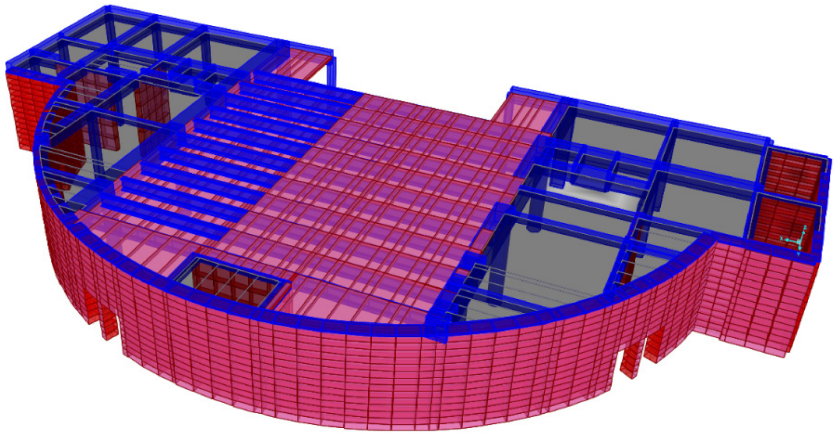

Figure 6. Three-dimensional view of the model.

The beams and columns were modeled with frame (mono-dimensional) elements, while shell (two-dimensional) elements were used for the slab of the steel-concrete floor and for the boundary wall. Regarding the constraint conditions, the nodes at foundation were restrained while the steel beams of the composite floor were released at the ends to simulate the on-site support condition. The masses were directly associated with the structural elements according to the density and geometric dimensions; a uniform area mass was assigned to the floors according to their weight. In addition to the dead loads of the elements, another permanent load equal to 9.78 kN/m^2 was assigned to the floors to take into account the filling and the weight of the flowerbeds. Instead, to simulate the live load, a constant load of 4 kN/m^2 was considered.

The capacity of the materials was defined considering the strength measured by the tests in situ, the knowledge level, and suitable partial safety factors. The concrete and steel strength values are, respectively, f_{cd} = 20.4/1.35 = 15 MPa and fyd = 306.7 MPa. Furthermore, a partial safety factor for the concrete equal to 1 and 1.5, respectively, for bending and shear stresses was applied. For the masonry, the experimental compressive strength was divided by FC = 1.2 and a partial safety factor of γ_M = 3 in the case of gravity loads and γ_M = 2 in the case of seismic assessment. The verification was carried out according to the provisions of the Italian Building Code [8] that are the same as Eurocode 8 [9].

A linear static analysis for gravity loads at the ultimate limit state (ULS) and a linear dynamic analysis with response spectrum for the seismic assessment of the life-safety limit state (SLV) were developed by the numerical model. The choice of the type of analysis for the seismic assessment depends on the characteristics of the building, which is irregular in plan and lacks ductile elements, but also on the low level of knowledge of the construction details. As a first step, the case study was analyzed for gravity loads, considering the building's self-weight, and the live loads. In Figure 7, the vertical compressive stresses in the boundary wall are reported, giving a maximum value of 0.23 MPa, which is lower than the strength (0.35 MPa).

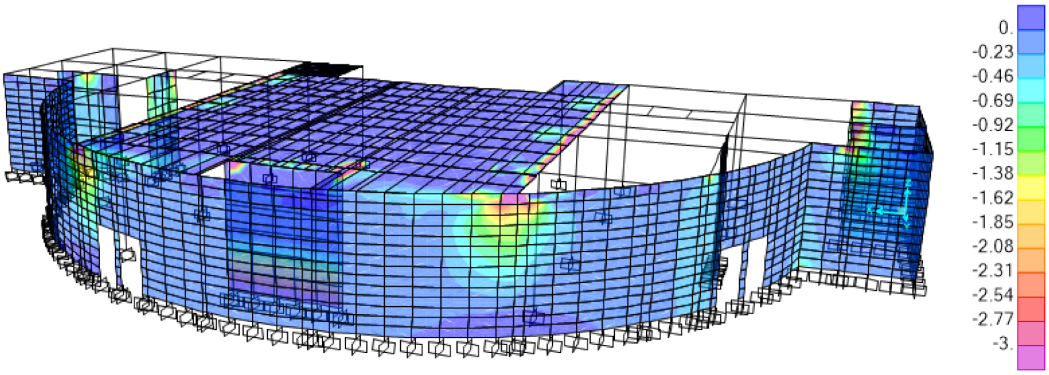

Figure 7. Maximum normal compression stresses in the boundary wall of the building (N/mm^2).

Before the seismic assessment, a modal analysis was carried out to study the dynamic response of the structure, i.e., periods of vibration, modal shapes, and modal participating mass ratios.

The linear dynamic analysis with response spectrum was implemented, combining the actions along the three main directions: X, Y, and Z.

Moreover, since the building has only one story, and the vertical resistant elements are not ductile due to poor construction details, the structure was considered to be non-dissipative, adopting a structural factor q of 1.5. In Figure 8, the percentage of the base reaction of RC walls and the masonry wall evaluated by numerical analysis are reported, evidencing the important role of the boundary ancient wall.

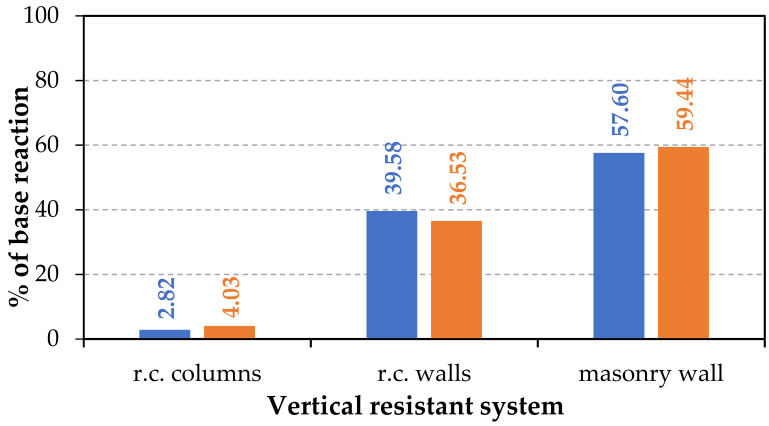

Figure 8. Percentage of base reaction of the vertical resistant systems.

The verification check of the structural elements was developed by evaluating the capacity/demand (C/D) ratio with respect to bending moment and shear. As expected, all the structural elements of the frames are safe (C/D > 1), while the RC walls are not always safe, with a minimum C/D of 0.15.

Regarding the masonry boundary wall, in this case, shear verification was not satisfied (C/D = 0.45); therefore, the seismic assessment of the building underlines the advisability of strengthening interventions both for the masonry and RC walls.

4. Energy Performance Assessment

The international standard UNI EN ISO 520001 [24] identifies three alternative methodologies for the building energy diagnosis: "asset", "design", and "tailored" ratings according to the aim of the investigation. When the final goal is a reliable simulation of a building, as in the proposed case study, the "tailored approach" has to be applied.

4.1. Building Plant System Characterization

The thermal transmittance (U) according to the methodology of UNI ISO EN 6946 [25] and the main dynamic parameters of periodic thermal transmittance (Y_{IE}), internal areal heat capacity (χ), decrement factor (f_a), and time lag (ϕ) was calculated according to UNI EN ISO 13786 [26]. The composition of the floors is described in Tables 2–4; however, according to the structural assessment for the vertical wall with known thicknesses, the other properties were determined on the basis of the materials' typology [22]:

- Circular masonry wall: 1. inner lime plaster (thickness 0.02 m, λ = 0.70 W/m K, c_p = 1000 J/kg K); 2. tuff block (thickness 0.70 m, λ = 0.55 W/m K, c_p = 1000 J/kg K); 3. outer reinforced plaster (thickness 0.03 m, λ = 0.90 W/m K, c_p = 1000 J/kg K);
- Plasterboard partitions facing the historic masonry wall: 1. inner lime plaster (thickness 0.02 m, λ = 0.70 W/m K, c_p = 1000 J/kg K); 2. plasterboard (thickness 0.08 m, λ = 0.21 W/m K, c_p = 1090 J/kg K).

The basement floor is characterized by a lightweight concrete slab with an overall thickness of 65 cm with the following properties: 1. stoneware (thickness 0.02 m, λ = 1.30 W/m K, c_p = 840 J/kg K); 2. cement mortar (thickness 0.03 m, λ = 1.40 W/m K, c_p = 1000 J/kg K); 3. concrete slab (thickness 0.10 m, λ = 0.33 W/m K, c_p = 1000 J/kg K); 4. preexisting rock (thickness 0.50 m, λ = 1.20 W/m K, c_p = 1000 J/kg K).

Table 5 shows the calculated stationary and dynamic parameters that give information on the energy quality of the building envelope. Clear double-glazed windows were considered, with an average thermal transmittance of 2.80 W/(m^2 K).

Table 5. Stationary and dynamic parameters of building envelope.

Envelope Components	U (W/m^2 K)	Y_{IE} (W/m^2 K)	f_a (-)	φ (h)	χ (kJ/m^2 K)
FLOOR A	1.12	0.008	0.007	>24	84.0
FLOOR B	1.57	0.052	0.033	19.3	97.5
FLOOR C	1.54	0.045	0.029	19.8	97.1
TUFF MASONRY WALL	0.66	0.003	0.005	>24	59.0
R.C. WALL	1.71	0.082	0.047	16.8	69.7
PARTITION	1.49	1.19	0.797	>24	48.5
BASEMENT	0.91	0.009	0.010	>24	59.4

For Italian Climatic Zone "C", the thermal transmittance must be lower than 0.36 W/m^2K: for the basement—0.38 W/m^2 K, for the floors—0.32 W/m^2 K, and for the partitions—0.80 W/m^2 K [5].

The comparison indicates that all components have a very low insulation level, and thus, high heat losses are expected. Instead, the dynamic parameters suggest that the massive structures have good behavior during the summer since the decrement factor is very low and the time delay due to the thermal mass is usually higher than 24 h.

It was difficult to find technical documentation of the subsystems in order to identify, for instance, thermal capacity, efficiency, energy efficiency ratios, and coefficients of performances of boilers and chillers. However, a standard air handling unit is installed; in the heating period, the pre- and post-heating batteries (efficiency of 86.4%) are fed by the natural gas boiler (capacity of 75 kW, efficiency 90%). The cooling dehumidification and post-heating operate during the summer. An air-to-water vapor compression chiller with a cooling capacity of 137 kW feeds the cooling and dehumidification coil with performance coefficient (COP) of 2.46, whereas the boiler feeds the post-heating coils. Other necessary information, such as the number, type, and location of heat terminals and air vents and the kind and lengths of distribution ducts and pipes, was checked during the surveys. All electricity of the conventional HVAC system is taken from the grid, and hot water is produced by the boiler.

The energy diagnosis indicated that there was no inefficient equipment, improper control schemes, or malfunctions concerning the building operation. The most critical element is the building envelope in terms of heat loss.

4.2. Dynamic Energy Simulation

All of the collected information allows for a definition of a three-dimensional model (Figure 9) for the resolution of the heat transfer under transient conditions through the building components.

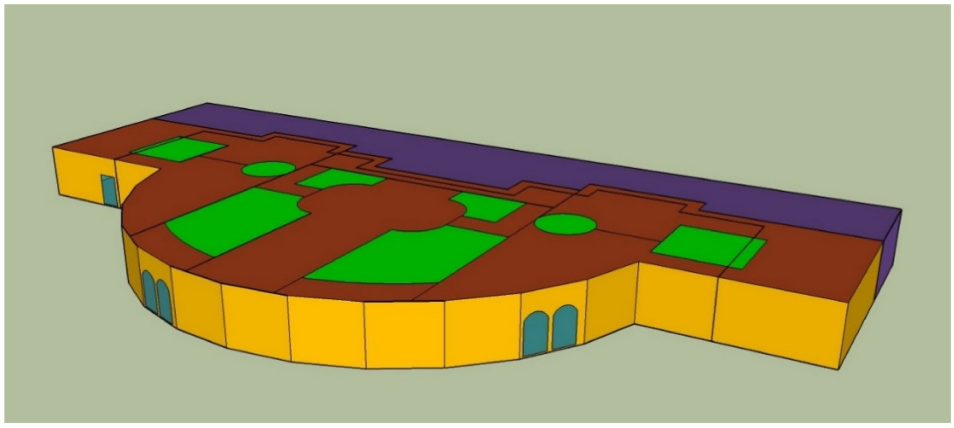

Figure 9. Rendering of simulated building.

The energy simulations with a one-minute timestep were performed through the use of "TRNSYS 18" [27] integrated with the Thermal Energy Systems Specialists (TESS) libraries [28].

The first step was the definition of the geomorphological details of the location. A specific weather file of Naples was used. In winter, the building is heated at 20 °C and in summer it is cooled at 26 °C with a relative humidity of 50% in both periods according to the scheduled occupancy. The processed mass flow is 2.74 kg/s with a recirculation factor of 0.516. An additional air change rate equal to 0.1 ACH was also considered because of the lack of air tightness when the ventilation system is turned off.

The most important TRNSYS types for the building plant system are listed in the following Table 6. The simulation models of the air handling unit elements were calibrated and validated with respect to experimental data in [29].

Table 6. Main parameters for the simulation model.

Simulation Models	Type	Library	Main Parameters
Building	56	Standard	As Table 5
Heating Coil	670	TESS	$c_{p,w}$: 4.19 kJ/kg K; ε: 0.864
Cooling Coil	508d	TESS	$c_{p,w}$: 4.19 kJ/kg K; f_{bp}: 0.177
Cross-Flow Heat Recovery	760	TESS	ε: 0.650
Humidifier	506a	TESS	ε_{Sat}: 0.551
Fun	644	TESS	$\dot{m}_{air}$: 2.74 kg/s
Pump	110	Standard	$\dot{m}_w$: 6.5 kg/s (chiller), 1.55 kg/s (boiler)
Natural Gas Boiler	700	TESS	$\dot{Q}_B$ = 75.0 kW η_B: 90%
Air-Cooled Chiller	655	TESS	$\dot{Q}_{CH}$: 137 kW Rated COP: 2.46

The main equations used in the simulation model are summarized in the following lines:

- Heating Coil

The heating coil model calculates the maximum heat transfer between the hot fluid (water heated up by the boiler) and the cold air as:

$$\dot{Q}_{max} = C_{min}(T_{w,in} - T_{air,in}) \quad (1)$$

where C_{min} is the minimum thermal capacitance between water and air, and $T_{w,in}$ and $T_{air,in}$ are the temperatures of water and air, respectively, entering in the heat exchanger. Then, the real heat that can be transferred between the fluids ($\dot{Q}_{HC}$) is determined through the efficiency of the coil (ε).

- Cooling Coil

This model follows the bypass approach, which means that the air stream is assumed to exit the coil at the average temperature between the inlet and saturated (at cold water temperature) conditions. The heat transfer from the air to the fluid is calculated as:

$$\dot{Q}_{CC} = \dot{m}_{air}\left(1 - f_{bp}\right)(h_{air,out} - h_{air,in}) - \dot{m}_{cond}h_{cond} \quad (2)$$

where $\dot{m}_{air}$ is the air mass flow rate, and $\dot{m}_{cond}$ is the condensing water; f_{pb} is the bypass factor; and h_{cond} is the enthalpy of the condensed water.

- Cross-Flow Heat Recovery

The heat exchanger allows two air flows to thermally interact. The thermal energy transferred from the warm air to the cold one is evaluated considering the efficiency (ε) and the maximum heat transfer that takes into account the minimum thermal capacitance and the maximum temperature gradient. Once established, the heat transferred from the outlet conditions of the two air flows is evaluated on the basis of the energy balances referred to as the two heat exchanger sections. On the basis of the outlet conditions, the condensed vapor is verified and calculated.

- Humidifier

The humidifier is a sort of direct evaporative cooling system in which the absolute humidity of the humidified air stream is increased, while the temperature is reduced because a part of the energy content of the air goes to evaporating water from the media through which the air flow is passing. The saturation efficiency (ε_{Sat}) is the crucial parameter to determine the condition of the air at the component outlet.

- Boiler

This mathematical model considers the primary energy demand of the boiler according to the set point temperature ($T_{w,set}$) selected for the heated water and the system efficiency (η_B). The power necessary to heat up the water is calculated as:

$$\dot{Q}_{need} = \dot{m}_w c_{p,w}(T_{w,set} - T_{w,in}) \quad (3)$$

where $\dot{m}_w$ is the mass flowrate of the water, $c_{p,w}$ is its heat capacity, and $T_{w,in}$ is the temperature of the water entering the boiler.

If $\dot{Q}_{need}$ is lower than the rated power of the boiler ($\dot{Q}_B$), the water can be heated up to the set point; the heat transfer to the fluid is limited to $\dot{Q}_{need}$, and the partial load ratio can be assessed as $\dot{Q}_{need}/\dot{Q}_B$. Once the energy transferred to the fluid is calculated, the primary power needed to operate the boiler is assessed through the efficiency:

$$\dot{Q}_{fuel} = \frac{\min\left\{\dot{Q}_{need}, \dot{Q}_B\right\}}{\eta_B} \quad (4)$$

- Air-Cooled Electric Chiller

This mathematical model relies on a catalog data lookup method that predicts the performance of an air-cooled chiller operating with a vapor compression cycle. The data files compiled with manufacturers' information provide the chiller capacity ratio and the COP ratio for different values of chilled water set point temperatures and outdoor ambient temperatures, as well as the chiller fraction of the full load power for varying values of the part load ratio. By interpolating between the data in the aforementioned files, the type identifies the available capacity ($\dot{Q}_{cool,ava}$) and COP (COP_{ava}) in the current condition. The available cooling capacity is compared with the required capacity to reach the temperature selected for the chilled water:

$$\dot{Q}_{cool,req} = \dot{m}_w c_{p,w}(T_{ch,w,in} - T_{ch,w,set}) \quad (5)$$

where $T_{ch,w,in}$ and $T_{ch,w,set}$ are the temperature of the water to be cooled and the set point one, respectively.

If the partial load ratio (PLR), evaluated as the ratio between the required cooling demand and the available capacity, has higher results than the one it is set to, it assumes a value between 0 and 1. Therefore, the cooling load met is calculated as:

$$\dot{Q}_{met} = \begin{cases} \dot{Q}_{cool,req} \text{ if } 0 < PLR < 1 \\ \dot{Q}_{cool,ava} \text{ if } PLR = 1 \end{cases} \quad (6)$$

while the chiller power required is given by:

$$\dot{P}_{el} = \frac{\dot{Q}_{cool,ava}}{COP_{ava}} \cdot FFLP \quad (7)$$

where FFLP is the fraction of full load power that is interpolated in the data file on the basis of PLR.

Finally, the effective COP, the heat ejected into the air stream, and the chilled water outlet temperature are assessed as follows:

$$COP_{eff} = \frac{\dot{Q}_{met}}{\dot{P}_{el}} \quad (8)$$

$$\dot{Q}_{rej} = \dot{Q}_{met} + \dot{P}_{el} \quad (9)$$

$$T_{ch,w,out} = T_{ch,w,in} - \frac{\dot{Q}_{met}}{\dot{m}_w c_{p,w}} \quad (10)$$

TRNSYS models the thermal behavior of a building divided into different thermal zones throughout transfer functions. The air nodes, corresponding to the thermal zones, are the element on which energy balance is performed, taking into account the thermal interaction with the outdoor environment (transmission, sun radiation, infiltration, etc.) and the internal load (equipment, lighting, people, etc.).

In this case study, to define reliable thermal loads, two typologies of thermal zones were created. The main one was the auditorium: 200 seats with sensible and latent gains per occupants of 65 W and 35 W, respectively (seated—very light activity [30], internal loads of around 2.0 kW); the other was the toilet. The lighting power was set to 5.0 W/m^2 with LED lamps [31].

The results of the simulation model were used for evaluating the global energy quality of the building plant system and for deciding possible refurbishment strategies jointly with the results of structural analysis.

First, the ratio between the heat losses between the indoor and outdoor environment due to each element ($Q_{tr,i}$) and the total heat losses due to energy transmission ($Q_{tr,tot}$)

for the winter season were evaluated. Similarly, for the summer period, this ratio was calculated considering the heat gains due to transmission through the opaque and glazed irradiated surfaces and the total heat gains due to energy transmission. The results are reported in Figure 10.

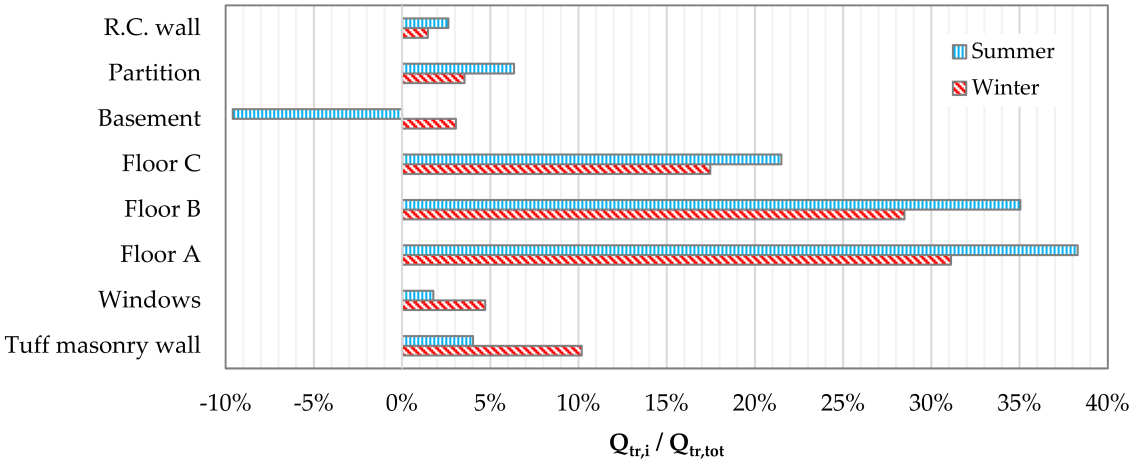

Figure 10. Weight of building elements on the transmission heat losses.

In both seasons, the most critical element was the roof; for instance, the floor A type had an incidence of 30% on the heating energy balance and of more than 35% on the summer energy balance. Regarding the summer behavior, the dynamic parameters indicate that the floors have adequate composition; however, for reducing the heat gains, the thermal mass should be further increased. This aspect is very important considering that on a typical summer day in Naples, the global solar radiation on the horizontal surface is higher than 900 W/m^2; this means that there is an important contribution of solar radiation on the opaque envelope, and its utilization is affected by thermal mass.

The tuff masonry wall impacted the winter losses by 10%; however, a very limited impact is attributable to the reinforced concrete wall due to the limited dispersing surface. However, an insulation intervention, if combined with structural works, can contribute to improving its characteristics. It must also be taken into account that the value of thermal transmittance of masonry wall is higher than the normative threshold, and thus it should be adequate.

However, the direct contribution of solar gains is negligible because the glazed surface is 23.6 m^2, whereas the opaque dispersing surface is 2196 m^2. For this reason, the design of an intervention for the windows is not convenient from an energetic point of view. Similarly, the basement is characterized by very low heat losses during the winter, whereas the negative percentage for the summer period indicates that it contributes to reducing the heat gains and thus helps to reduce the cooling needs. For these reasons, it was not necessary to evaluate the intervention for this component.

Finally, the dynamic simulation gives information on the primary energy consumption equal to 140.5 kWh/m^2. This result appears to be in good accordance with data reported in [32,33]. In more detail, the sensible energy need during the winter and summer period is, respectively, 17,314 kWh and 5824 kWh. These values are mainly related to the quality of the building envelope and confirm the results of the previous analysis. The refurbishment intervention should be focused mainly on the reduction of the heat losses because the thermal mass assures good summer performance. Moreover, the latent energy need is 4858 kWh and 18,927 kWh, respectively, for the winter and summer energy balance. This contribution is mainly due to the occupation rate, and only an intervention in the air-conditioning system can be decisive in its reduction.

5. Integrated Methodology for the Building Upgrading

The structural and energetic upgrading is addressed with a similar methodology that consists of identifying the role of each element that affects the performance. In particular, from the structural point of view they are the structural elements, i.e., masonry and RC walls, while on the energy side they are the building envelope components and equipment. When the contribution of each element is identified together with the possibility to improve it, the upgrading solution is defined. It is worth underlining that the structural interventions on the building envelope are economically advantageous because it is still necessary to upgrade the energy performance. In the following, two examples of upgrading are described, highlighting that the same methodology is applied.

5.1. Structural Upgrading

The approach used to identify the structural interventions was developed using the following methodology:

(1) Analyze the dynamic response of the building to detect any irregularities;
(2) Define the participation in the seismic resistance of the structure of each structural element;
(3) Define interventions, including the modification of existing elements and the introduction of new structural elements to improve the distribution of seismic actions and optimize the contribution of each element;
(4) Local strengthening of structural elements.

The analysis of the dynamic response of the structure shows a strong irregularity with a coupling of modes in the two main directions. Furthermore, it was evidenced that the main role is played by the RC and masonry walls, which absorb about the same percentage of seismic action in both the two principal directions. The verification check of the structural elements has shown that some RC walls are not safe for either shear or bending stresses. In particular, the most lacking is the RC wall "E", characterized by an "E" shape and a minimum C/D equal to 0.15 in bending. A large part of the masonry wall lacks shear stresses with a minimum value of C/D equal to 0.33.

The results suggest that a first step could be to regularize the dynamic behavior of the structure in order to better redistribute the stresses on the bearing elements. To this aim, firstly, the rigidity of the E-shaped RC wall was reduced by separating the rectangular components along the X and Y direction, and new RC and masonry structural elements were added.

The effect of such upgrading interventions is summarized in Table 7, in which the main periods and the participating mass ratios associated with each mode, the percentage of seismic action absorbed, and the C/D ratios are reported for each upgrading contribution.

Table 7. Main results of different structural interventions.

Structural Upgrading	Period [s] and Partecipating Mass Ratios (%)				Percentage of Base Reaction (%)			C/D Ratio					
	T	M Ux	M Uy	M Rz		r.c.	Masonry	r.c.	Bending	Shear	Masonry	Bending	Shear
Step 1: As-built	0.120	19	53	20	X	40	58	**W-A**	0.56	0.48	**M1**	1.99	1.12
								W-B	1.09	0.97	**M2**	1.92	0.33
								W-C	0.49	3.02	**M3**	4.77	0.62
	0.090	67	25	-				**W-D**	1.08	0.49	**M4**	2.87	0.80
								W-E	0.15	0.44	**M5**	2.63	0.45
	0.050	5	12	60	Y	37	59				**M6**	6.58	0.80
											M7	7.90	0.70

Table 7. *Cont.*

Structural Upgrading	Period [s] and Partecipating Mass Ratios (%)				Percentage of Base Reaction (%)			C/D Ratio					
	T	M Ux	M Uy	M Rz		r.c.	Masonry	r.c.	Bending	Shear	Masonry	Bending	Shear
Step 2: Splitting of the E-shape RC wall	0.130	26	45	20	X	35	61	**W-A**	0.55	0.47	**M1**	1.73	1.52
								W-B	1.15	1.01	**M2**	1.86	0.73
								W-C	0.68	2.15	**M3**	2.75	1.08
	0.090	55	35	-				**W-D**	1.27	0.42	**M4**	2.51	1.30
					Y	39	58	**W-E1**	0.43	0.60	**M5**	5.19	0.57
								W-E2	0.61	0.61	**M6**	6.39	0.76
	0.050	3	5	21				**W-E3**	0.54	0.71	**M7**	14.17	0.74
								W-E4	1.28	0.87			
Step 3: Addition of a new RC wall	0.095	85	-	4	X	38	58	**W-A**	1.88	1.79	**M1**	2.42	0.98
								W-B	1.10	0.87	**M2**	5.01	0.70
								W-C	0.67	2.97	**M3**	2.62	0.72
	0.070	-	90	-				**W-D**	0.99	0.54	**M4**	2.66	0.85
					Y	52	38	**W-E1**	0.61	0.85	**M5**	10.94	0.80
								W-E2	0.80	0.79	**M6**	7.00	0.83
	0.040	3	-	67				**W-E3**	0.69	0.86	**M7**	9.88	0.59
								W-E4	1.20	0.60			
Step 4: Addition of a new masonry wall made by brick blocks with integrated insulation	0.076	76	11	2	X	34	56	**W-A**	2.26	1.92	**M1**	3.53	1.28
								W-B	1.26	1.30	**M2**	5.39	0.79
								W-C	1.56	3.30	**M3**	2.63	0.80
	0.074	12	70	-				**W-D**	1.64	0.89	**M4**	3.40	1.12
					Y	52	37	**W-E1**	1.13	1.23	**M5**	11.61	1.00
								W-E2	1.33	1.14	**M6**	6.83	1.05
	0.05	1	-	26				**W-E3**	1.29	2.10	**M7**	17.54	0.87
								W-E4	1.57	0.75			
Step 5: Local strenghtening with FRP and FRCM	0.076	76	11	2	X	34	56	**W-A**	2.26	1.92	**M1**	3.53	1.98
								W-B	1.26	1.30	**M2**	5.39	1.33
								W-C	1.56	3.30	**M3**	2.63	1.33
	0.074	12	70	-				**W-D**	1.64	1.28	**M4**	3.40	1.72
					Y	52	37	**W-E1**	1.13	1.23	**M5**	11.61	1.38
								W-E2	1.33	1.14	**M6**	6.83	1.45
	0.050	1	-	26				**W-E3**	1.29	2.10	**M7**	17.54	1.04
								W-E4	1.57	1.03			

It can be observed that the cut of the E-shaped RC wall did not change the dynamic behavior of the structure but led to an improvement in bearing capacity, enhancing the minimum C/D ratio of the RC walls from 0.15 to 0.43 due to a redistribution of the stresses among the walls.

In the second step, a new RC wall (thickness equal to 0.5 m) was added on the left side of the structure along the Y direction (see Figure 11). In this way, the structure obtains a more regular dynamic behavior; indeed, two predominantly translational modes along the two main directions can be identified. A further improvement in the verification checks for bending (C/D minimum is 0.61) and shear (C/D minimum is 0.5) for both RC and masonry walls was achieved.

In the third step, new masonry walls (see fourth line of Table 7) characterized by brick blocks (30 cm) with integrated thermal insulation were added along the X direction at the side opposite to the ancient masonry wall. This solution allowed us to save all the RC walls for bending moment and to increase the C/D ratio for shear from 0.5 to 0.6 for the RC walls and from 0.59 to 0.87 for the ancient masonry wall. It is worth underlining that this solution also contributes to energy upgrading.

Finally, the local strengthening of the structural elements still lacking was designed, taking into account that, especially for the masonry boundary wall, a widespread structural solution integrates well with the wall's thermal insulation, necessary to improve the energetic performance. In particular, to increase the in-plane shear capacity of masonry walls, the FRCM strengthening system was adopted because it is an efficient solution to improve the global response of the wall without increasing its stiffness [34].

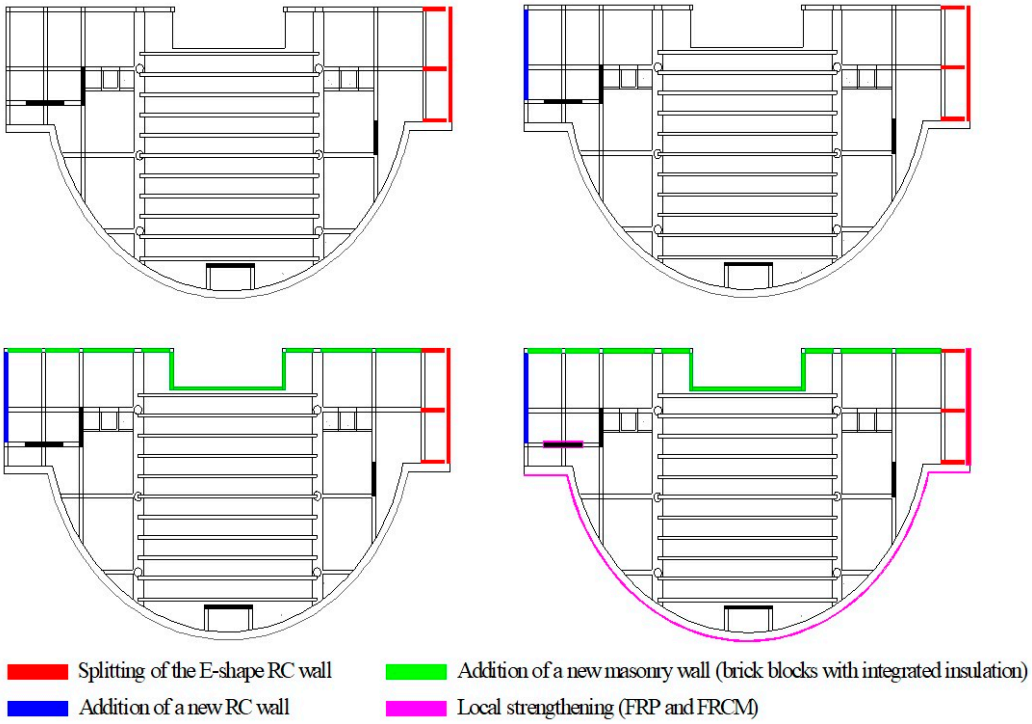

Figure 11. Schematic representation of the structural interventions from step 2 to 5.

In particular, the strengthening intervention was designed according to the Italian CNR DT 215 guideline [35], using a theoretical approach to define the factor for the amplification of the strength since the masonry is thicker than 400 mm. Full coverage with an FRCM system made of a glass grid was chosen. In particular, to obtain the necessary increment of the shear capacity, two layers with a thickness of 0.025 mm of commercial fibers (with Young modulus and strain equal to 1000 MPa and 0.8%, respectively) were employed. After the strengthening of the masonry boundary wall, all the C/D ratios for shear were higher than 1.

The RC walls W-D and W-E4, which are not safe for shear, were strengthened with FRP composite materials according to the provisions reported in the Fib Bulletin [36] and the Italian CNR DT 200 guidelines [37]. In particular, the retrofitting included unidirectional strips of carbon fiber both in the longitudinal and transversal directions laid on the two sides of the panel, connected to each other by double-staple passing connectors (spikes) at the wall's connections. The strips have a width of 200 mm and a thickness of 0.189 mm. The two longitudinal strips were arranged with a distance of 20 cm from the wall ends, while the horizontal strips were arranged at a distance of 800 mm. Due to the use of metal connectors, the deformation and the design stress for delamination of the composite material were equal to 3‰ and 690 MPa, respectively.

5.2. Energy Upgrading

In this case, two retrofit scenarios can be investigated. In the first one, the potential of each single retrofit technology is evaluated for understanding the role of each element on the improvement of the energetic performance. In the second scenario, the combination of the preferable retrofit actions, and thus the most profitable according to the calculated efficiency, is considered.

According to some important criticalities identified during the audit phase, some energy efficiency measures were investigated:

- Wall insulation: application of 5 cm of wooden fiber insulation (density = 160 kg/m^3; λ = 0.038 W/m K, cp = 2100 J/kg K) on the external side of the tuff masonry wall (TM) and 10 cm on the reinforced concrete wall (RCW);

- Floor insulation: application of panels of extruded polystyrene insulation (density = 35 kg/m^3; λ = 0.035 W/m K, cp = 1450 J/kg K) with a thickness of 10.0 cm for floor B (FB) and floor C (FC) and 8.0 cm for floor A (FA);
- Partition insulation (PI): installation of brick blocks (30 cm) with integrated insulation (λ = 0.06 W/m K, cp = 1000 J/kg K);
- Heat recovery unit (HR): installation of cross-flow heat recovery unit (efficiency 0.65) that allows heat recovery without any contact, direct or not, between the air fluxes.

Table 8 proposes the results of the sensitivity analysis on the incidence of each intervention on the energy performance. In more detail, the following parameters were calculated: the variation of the insulation level (ΔU); the variation of thermal inertia (ΔY_{IE}); the weight of reduction of heat losses for transmission during the winter ($\Delta Q_{tr,winter}$) and summer ($\Delta Q_{tr,summer}$) of the i-component with respect to the global variation of the heat losses for transmission; the total primary energy saving (ΔEP); and the reduction in the sensible (ΔE_s) balance during summer and winter.

Table 8. Sensitivity analysis of refurbishment intervention.

Interventions	ΔU	ΔY_{IE}	$\Delta Q_{TR,WINTER}$	$\Delta Q_{TR,SUMMER}$	$\Delta E_{S,WINTER}$	$\Delta E_{S,SUMMER}$	ΔEP
TM	−45%	−87%	−7%	−2%	−6.8%	−6.0%	−0.8%
RCW	−82%	−96%	−2%	−2%	−1.7%	−0.5%	−0.4%
PI	−88%	−99%	−5%	−7%	−7.1%	+20%	−2.1%
FA	−71%	−95%	−33%	−34%			
FB	−78%	−94%	−33%	−34%	−47%	−56%	−4.3%
FC	−78%	−96%	−20%	−21%			

The proposed indicators suggest that the interventions are able to improve the performance of all building components, with the lowest impact on the tuff masonry wall. However, in order to understand the weight of each element in the refurbishment design, $\Delta Q_{tr,winter}$ and $\Delta Q_{tr,summer}$ must be analyzed. With reference to the winter season, $\Delta Q_{tr,winter}$ is the ratio between the difference of the losses due to thermal transmission on the building component before and after the refurbishment and the difference of the total thermal losses before and after the refurbishment on all elements. Similarly, $\Delta E_{S,WINTER}$ indicates the variation of the sensible heat load compared with the base case. The analysis of Table 8 suggests, once again, that the most important intervention, considering the energy balance, is the floor insulation, since ΔE_s is equal to −47% and −56%, respectively, in the winter and summer season. The insulation of the tuff wall reduced the sensible load by around -6.8% during the winter and −6.0% during the summer. The case of insulated brick blocks on the partition gave different results because it reduced the sensible load during the winter but increased the summer heat load. When the primary energy saving is considered, the contribution of the walls is negligible, whereas with the roof insulation, this reduction was −4.3%.

If all interventions are applied, ΔEP becomes −7.8%. Since the energy refurbishment is designed together with the structural restoration that is focused mainly on the wall, it is profitable to consider all interventions even if the analysis of the single efficiency measure has indicated low energy savings.

Moreover, it must be considered that the results in terms of primary energy are affected by the weight of the latent load due to the type of building use. For this reason, the installation of a heat recovery unit was also considered for improving the whole building plant performance. Briefly, considering the base case with the application of the HR, the primary energy saving was −16%. This result allows the underlining of another important aspect of the proposed research. In buildings with all-air systems, due to the high level of occupancy, significant air flows are treated; thus, the intervention on the plants seems to have a predominant weight in terms of primary energy savings. However, the refurbishment of the building envelope, as demonstrated, is always convenient when considering all possible points of view, and thus leads to energy savings, better indoor microclimate, reduction of polluting emissions, and technical and economic feasibility.

Indeed, the renovation of the building envelope stabilizes the indoor microclimate in the winter. In particular, higher thermal insulation reduces the indoor fluctuations of temperature and relative humidity by increasing the thermal resistance and inertia of the envelope. Moreover, a lower dynamic thermal transmittance induces more comfortable indoor temperatures during the cooling period. For this reason, the last investigated scenario concerns the application of both envelope efficiency measures and heat recovery installation. In this case, the ΔEP became −18%.

5.3. Discussion on the Cost-Benefit of the Integrated Approach

The detailed analysis of the construction has shown that it is very deficient both in terms of energy and seismic performance. Therefore, an integrated approach to upgrading the building performance for both aspects is strictly necessary in order to avoid economic loss from two points of view. The first economic optimization is due to the cost reduction by carrying out the work at the same time and in the same site with construction finishes such as plaster and painting, which are necessary for the insulation and strengthening of the existing and new masonry walls.

In order to evaluate the economic feasibility and to have a frame for a conceptual discussion on the proposed integrated approach, the relative costs of each retrofitting choice have been estimated. Furthermore, it is important to identify a reference value of the building, which can be approximately 2,700,000 EUR assuming a market value of 3000 EUR/m^2.

Table 9 reports the investment costs (CI) derived primarily from a market-based analysis. Note that all costs have to be considered as indicative since the purpose is simply to allow a discussion about energy or seismic-only retrofitting versus integrated ones.

As shown in Table 9, the total costs for the single energy and structure upgrading are 149,657 EUR and 151,610 EUR, respectively. Thus, if these interventions are carried out separately at different times, an overall cost of 301,180 EUR is achieved, that is, 11% of the building value (6% for the energy and 5% for the structural upgrade, respectively). Instead, by adopting an integrated approach in designing both an energy and structural retrofit solution, a total cost of 272,200 EUR is achieved, saving up to 10% (1% of the building value), but further savings that were not considered in this analysis, due to the organization of the same construction site and the time required, could be double.

Table 9. Investment costs for sole energy, sole structure, and integrated interventions.

	Energy		**Structure**		**Integrated**	
	CI	**Total Cost**	**CI**	**Total Cost**	**CI**	**Total Cost**
Existing masonry wall	80 EUR/m^2	22,800 EUR	230 EUR/m^2	131,250 EUR	270 EUR/m^2	142,600 EUR
New masonry wall *	80 EUR/m^2	22,400 EUR	68 EUR/m^2	19,070 EUR	90 EUR/m^2	25,200 EUR
Roof	107 EUR/m^2	96,500 EUR	-	-	-	-
Heat recovery unit	4500 EUR	4500 EUR	-	-	-	-
RC walls	80 EUR/m^2	3370 EUR	175 EUR/m^2	1290 EUR	215 EUR/m^2	3400 EUR
All		**149,657 EUR**		**151,610 EUR**		**272,200 EUR**

* When only an energy upgrade is performed, the wall is realized with an insulating block without a structural role; conversely, when only a structural upgrade is carried out, no insulating blocks are used.

The second grounds of appeal for carrying out the integrated interventions, less evident to technicians and administrators but more important than the savings in the work costs, is the economic loss or savings during the life of the construction if only one of the two performance areas is upgraded with the other lacking.

First, in Table 10, for the various interventions of the energy retrofitting, the exercise costs "CE" for heating, cooling, and ventilation are reported by considering the natural gas and electricity tariffs from "The Regulatory Authority for Electricity and Gas" of Italy [38], and these include regional and national taxes. In particular, the cost for the natural gas is 0.80 EUR/Nm^3, and the electricity cost is 0.20 EUR/kWh_{el}.

Table 10. Exercise costs.

Interventions	CE (EUR)	ΔCE
EXISTING MASONRY AND RC WALLS	14,421	−0.82%
NEW MASONRY WALLS	14,334	−1.45%
ROOF	14,109	−3.0%
HEAT RECOVERY UNIT	13,790	−5.20%
ALL	12,374	−15%

The reduction in the exercise cost "ΔCE" can be evaluated considering that the base case is characterized, according to the simulation schedules, by expenses for annual energy management of 14,545 EUR. It is worth noting that the overall saving of 15% is due to all the energy retrofitting interventions, and the largest contribution is due to the heat recovery unit.

If only the energy performance of the building is improved, overall savings of 15% of the energy cost would be achieved (that is, 12,374 EUR/year), which gives a cost saving of 25% of the building value in 50 years (the nominal life of the building) with an investment cost of 6% of the total cost of the building.

Despite the positive aspect of energy saving to assess the convenience of the intervention over time, it should be considered that, from a structural point of view, if structural upgrading is not carried out, the structure could suffer significant damage during an earthquake. Furthermore, if an earthquake, also much lower than the designed one at the ultimate limit state, happens, the structure will be damaged, with loss of the investment for the energy intervention; this means that the economic loss would increase to 6% of the building value.

Instead, if an integrated refurbishment solution is employed, the investment cost would be 299,606 EUR, which corresponds to 11% of the total cost of the building, but in case of an earthquake, the damage and the loss, to both economic and human health, would be reduced, also saving the investment for the energy upgrade.

The simple analysis presented in this section, even if not all economic parameters have been considered or detailed, can give a significant example of the importance of integrated intervention considering the economic point of view, more so than the combined aspects of safety (structural performance) and comfort (energy performance).

6. Conclusions

The need to improve the performance of existing public buildings both for seismic capacity and energy consumption is growing in Italy and in other countries which face seismic activity. However, the topic of the combined evaluation of structural and energy performance is worthy of investigation. By means of a case study, this paper suggests a complete methodology that allows investigation into energy and structural behavior of a building with the same formal and applicative approach. This can be summarized in the following steps:

- The in situ investigation was finalized to assess the material/structural and the thermal/energy characteristics of the building alongside a complete survey and tests;
- Defining the structural and energy simulation models for studying the weight of the building and plant components on the whole performance;
- Analysis of technical measures for improving both the structural and energy performances step by step, considering the role of the various interventions both in terms of performance improvement and cost and loss aspects.

The application of this approach in the case study has allowed us to identify the perimeter masonry wall as the common key element for improving the overall performance, as well as other elements such as the specific importance of energy saving (the roof) or structural contribution (internal RC walls). The strengthening and the thermal insulation of the perimeter masonry wall was identified together with the construction of a new masonry

wall as a factor that contributes to the seismic bearing capacity and gives a further boundary condition for the thermal insulation of the envelope, not with a properly convenient effect. Moreover, the application of 8—-10 cm of extruded polystyrene insulation was also considered for the floors and the installation of a heat recovery unit for improving the performance of the installed all-air system. In the complete refurbished configuration, the energy demand was reduced by 18%. The cost for the integrated intervention allows a saving of 10% considering only the works, but this benefit can be largely amplified by adding the reduction of the time and site organization; furthermore, the importance of post-earthquake loss cannot be neglected. Therefore, further case studies and a generalized method used to optimize the integrated interventions are still necessary, with a more detailed analysis of the costs and post-earthquake loss.

Author Contributions: Conceptualization, M.R.P.; methodology, R.F.D.M. and A.D.A.; software, A.D.A. and F.T.; validation, M.R.P., R.F.D.M. and F.T.; formal analysis, A.D.A. and F.T.; writing—original draft preparation, A.D.A. and R.F.D.M.; writing—review and editing, F.T.; supervision, M.R.P. All authors have read and agreed to the published version of the manuscript.

Funding: This research was carried out within the framework of Reluis research project 2019–2021 Wp5 task 5.1.

Institutional Review Board Statement: Not applicable.

Informed Consent Statement: Not applicable.

Acknowledgments: The authors acknowledge PON Research and Innovation 2014–2020, Axis I-Investments in Human Capital, MIUR notice AIM—"International Attraction and Mobility"—Line 1, Project: AIM 1823125-3—Cultural Heritage that financed the research of Alessandra De Angelis, and Arch. Liana De Filippis for her support in finding the historical information and carrying out surveys and tests in situ; we further acknowledge Francesco Santamato for his support with the structural modeling.

Conflicts of Interest: The authors declare no conflict of interest.

Nomenclature

ag	ground acceleration
CE	Cost of Exercise (EUR/y)
CI	Cost of Investment (EUR) or (EUR/m^2)
C	Thermal Capacitance (kJ/s K)
COP	Coefficient of Performance (-)
c_p	Specific Heat (kJ/kg K)
Cu	Usage coefficient
C/D	capacity/demand ratio
f_a	Decrement factor (-)
f_{bp}	Bypass factor (-)
f_{cd}	Compressive concrete strength (MPa)
FFLP	Fraction of Full Load Power (-)
f_{yd}	Steel yielding strength (MPa)
F0	Maximum amplification factor
h	Enthalpy (kJ/kg)
$\dot{m}$	Mass flow rate (kg/s)
M_Ux	Modal participating mass ratio in X direction
M_Uy	Modal participating mass ratio in Y direction
M_Uz	Modal participating mass ratio in Z direction
$\dot{P}$	Power (kW)
PLR	Partial Load Ratio (-)
$\dot{Q}$	Heat transfer or Capacity (kW)
R	Thermal Resistance (m^2 K/W)
T	Temperature (°C) or (K)
TR	Return period (y)

U	Thermal transmittance (W/m^2K)
Y_{IE}	Periodic thermal transmittance (W/m^2K)
Greek symbols	
ΔCE	Reduction of the Exercise Cost (%)
ΔEP	Total Primary Energy Saving (%)
ΔE_s	Reduction of the Sensible Load (%)
ΔQ_{tr}	Reduction of Heat Losses for Transmission (%)
ΔU	Variation of the insulation level (%)
ΔY_{IE}	Variation of thermal inertia (%)
ε	Efficiency (-)
η	Efficiency (-)
λ	Thermal conductivity (W/m K)
ϕ	Time lag (h)
χ	Internal areal heat capacity (kJ/m^2 K)
ω	Humidity ratio (kg_{vapor}/kg_{air})
Subscripts	
air	Air
ava	Available
B	Boiler
CFHR	Cross-Flow Heat Recovery
CH	Chiller
ch	Chilled
cold	Cold
cond	Condensed vapor
cool	Cooling
el	Electric
fuel	Of the Fuel
HC	Heating Coil
i	i-th element
in	Inlet
max	Maximum
met	Load Met
min	Minimum
mix	Mixing condition
need	Necessary
out	Outlet
rej	Rejected
req	Required
Sat	Saturation
set	Set point
summer	During summer
tot	Total
w	Water
warm	Warm
wb	Wet Bulb
winter	During winter
Acronyms	
FA	Floor Type A
FB	Floor Type B
FC	Floor Type C
INAF	National Institute of Astrophysics
PI	Partition Insulation
RC	Reinforced Concrete
RCW	Reinforced Concrete walls
SLV	Life-Safety Limit State
S/V	Surface-to-Volume ratio
TM	Tuff Masonry
ULS	Ultimate Limit State

References

1. Directive 2018/844/EU of the European Parliament and of the Council of 30 May 2018 amending Directive 2010/31/EU on the energy performance of buildings and Directive 2012/27/EU on energy efficiency. *Off. J. Eur. Union* **2018**, L156/75–L156/91.
2. Assimakopoulos, M.-N.; Papadaki, D.; Tariello, F.; Vanoli, G.P. A Holistic Approach for Energy Renovation of the Town Hall Building in a Typical Small City of Southern Italy. *Sustainability* **2020**, *12*, 7699. [CrossRef]
3. Assimakopoulos, M.-N.; De Masi, R.F.; Fotopoulou, A.; Papadaki, D.; Ruggiero, S.; Semprini, G.; Vanoli, G.P. Holistic approach for energy retrofit with volumetric add-ons toward nZEB target: Case study of a dormitory in Athens. *Energy Build.* **2020**, *207*, 109630. [CrossRef]
4. Hong, Y.; Ezeh, C.I.; Deng, W.; Hong, S.-H.; Ma, Y.; Tang, Y.; Jine, Y. Coordinated energy-environmental-economic optimisation of building retrofits for optimal energy performance on a macro-scale: A life-cycle cost-based evaluation. *Energy Conv. Manag.* **2021**, *243*, 114327. [CrossRef]
5. Gazzetta Ufficiale. *Ministerial Decree—DECRETO 26 Giugno 2015 Applicazione Delle Metodologie di Calcolo Delle Prestazioni Energetiche e Definizione Delle Prescrizioni e dei Requisiti Minimi Degli Edifici*; GU n.162 del 15-7-2015-n. 39; Gazzetta Ufficiale: Rome, Italy, 2015. (In Italian)
6. Balleri, A.; Marini, A. Does seismic risk affect the environmental impact of existing buildings? *Energy Build.* **2016**, *110*, 149–158. [CrossRef]
7. Gazzetta Ufficiale. *Ordinance of the Council of Ministers OPCM n. 3274 (20-03-2003). Primi Elementi in Materia di Criteri Generali per la Classificazione Sismica Del Territorio Nazionale e Normative Tecniche per le Costruzioni in Zona Sismica*; G.U. n. 105 del 8/05/2003; Gazzetta Ufficiale: Rome, Italy, 2003. (In Italian)
8. Ministerial Decree of Public Works (M.D.) (14/01/2008). *New Technical Codes for Constructions*; n. 29 (4/2/2008); Gazzetta Ufficiale: Rome, Italy, 2008.
9. CEN. Eurocode 8—EN 1998-3. Design of structures for earthquake resistance. In *Part 3: Assessment and Retrofitting of Buildings*; CEN: Brussels, Belgium, 2005.
10. Caverzan, A.; Lamperti Tornaghi, M.; Negro, P. A Roadmap for the Improvement of Earthquake Resistance and Eco-Efficiency of Existing Buildings and Cities. In Proceedings of SAFESUST Workshop; JRC, JRC Science Hub: Ispra, Italy, 2015; pp. 1–136.
11. Bournas, D.A. Concurrent Seismic and Energy Retrofitting of RC and Masonry Building Envelopes Using Textile-Based Composites Combined with Insulation Materials: A New Concept. *Compos. Part B* **2018**, *148*, 166–179. [CrossRef]
12. Artino, A.; Evola, G.; Margani, G.; Marino, E.M. Seismic and Energy Retrofit of Apartment Buildings through Autoclaved Aerated Concrete (AAC) Blocks Infill Walls. *Sustainability* **2019**, *11*, 3939. [CrossRef]
13. Triantafillou, T.C.; Karlos, K.; Kefalou, K.; Argyropoulou, E. An innovative structural and energy retrofitting system for URM walls using textile reinforced mortars combined with thermal insulation: Mechanical and fire behavior. *Constr. Build. Mater.* **2017**, *133*, 1–13. [CrossRef]
14. Ascione, F.; Ceroni, F.; De Masi, R.F.; de' Rossi, F.; Pecce, M.R. Historical buildings: Multidisciplinary approach to structural/energy diagnosis and performance assessment. *Appl. Energy* **2017**, *185*, 1517–1528. [CrossRef]
15. De Angelis, A.; Ascione, F.; De Masi, R.F.; Pecce, M.R.; Vanoli, G.P. A novel contribution for resilient buildings. Theoretical fragility curves: Interaction between energy and structural behavior for reinforced concrete buildings. *Buildings* **2020**, *10*, 194. [CrossRef]
16. Menna, C.; Del Vecchio, C.; Di Ludovico, M.; Mauro, G.M.; Ascione, F.; Prota, A. Conceptual design of integrated seismic and energy retrofit interventions. *J. Build. Eng.* **2021**, *38*, 102190. [CrossRef]
17. Marini, A.; Passoni, C.; Belleri, A.; Feroldi, F.; Preti, M.; Metelli, G.; Riva, P. Combining Seismic Retrofit with Energy Refurbishment for the Sustainable Renovation of RC Buildings: A Proof of Concept. *Eur. J. Environ. Civ. Eng.* **2017**, 1–21. [CrossRef]
18. Mastroberti, M.; Bournas, D.; Vona, M.; Manganelli, B.; Palermo, V. Combined seismic plus energy retrofitting for the existing rc buildings: Economic feasibility. In Proceedings of the 16th European Conference on Earthquake Engineering, Tessaloniki, Greece, 18–21 June 2018.
19. De Angelis, A.; Maddaloni, G.; Pecce, M.R. Seismic vulnerability assessment of a monumental masonry building. *Infrastructures* **2020**, *5*, 93. [CrossRef]
20. ISO. *UNI 10351:2015: Building Materials and Products—Hygrothermal Proprieties—Procedure for Determining the Design Values*; ISO: Geneva, Switzerland, 2015.
21. Peel, M.C.; Finlayson, B.L.; McMahon, T.A. Updated world map of the Köppen–Geiger climate classification. *Hydrol. Earth Syst. Sci.* **2007**, *11*, 1633–1644. [CrossRef]
22. Available online: https://en.climate-data.org/europe/italy/campania/naples-4561/ (accessed on 16 June 2021).
23. Computers and Structures. *SAP2000 Version 18*; Computers and Structures: Walnut Creek, CA, USA, 2016.
24. ISO. *UNI EN ISO 52000-1:2018: Energy Performance of Buildings—Overarching EPB Assessment—Part 1: General Framework and Procedures*; ISO: Geneva, Switzerland, 2018.
25. ISO. *UNI EN ISO 6946:2018: Building Components and Building Elements—Thermal Resistance and Thermal Transmittance—Calculation Methods*; ISO: Geneva, Switzerland, 2018.
26. ISO. *UNI EN ISO 13786:2018: Thermal Performance of Building Components—Dynamic Thermal Characteristics—Calculation Methods*; ISO: Geneva, Switzerland, 2018.
27. TRNSYS, The Transient Energy System Simulation Tool. Available online: http://www.trnsys.com (accessed on 1 June 2021).

28. Thermal Energy System Specialists. *Thermal Energy System Specialists Components Library v. 17.01*; Thermal Energy System Specialists: Madison, WI, USA, 2004.
29. Angrisani, G.; Roselli, C.; Sasso, M. Experimental validation of constant efficiency models for the subsystems of an unconventional desiccant-based Air Handling Unit and investigation of its performance. *Appl. Therm. Eng.* **2012**, *33*, 100–108. [CrossRef]
30. ISO. *UNI EN ISO 7730:2006: Ergonomics of the Thermal Environment—Analytical Determination and Interpretation of Thermal Comfort Using Calculation of the PMV and PPD Indices and Local Thermal Comfort Criteria*; ISO: Geneva, Switzerland, 2006.
31. *UNI EN 15193-1:2017: Energy Performance of Buildings—Energy Requirements for Lighting—Part 1: Specifications, Module M9*; Slovenian Institute for Standardization: Ljubljana, Slovenia, 2017.
32. Mahdi Salehi, M.; Cavka, B.T.; Frisque, A.; Whitehead, D.; Bushe, W.K. A case study: The energy performance gap of the Center for Interactive Research on Sustainability at the University of British Columbia. *J. Build. Eng.* **2015**, *4*, 127–139. [CrossRef]
33. Filippín, C.; Beascochea, A. Performance assessment of low-energy buildings in central Argentina. *Energy Build.* **2007**, *39*, 546–557. [CrossRef]
34. D'Ambra, C.; Lignola, G.P.; Prota, A. Simple method to evaluate FRCM strengthening effects on in-plane shear capacity of masonry walls. *Constr. Build. Mater.* **2021**, *268*, 121125. [CrossRef]
35. CNR DT 215. *Guide for the Design and Construction of Fiber Reinforced Inorganic Matrix Systems for Strengthening Existing Structures*; Italian Council of Research (CNR): Rome, Italy, 2018.
36. FIB. *Externally applied FRP Reinforcement for Concrete Structures*; FIB Bulletin: Lausanne, Switzerland, 2019; p. 229.
37. CNR-DT 200. *Instructions for the Design, Execution and Control of Static Consolidation Interventions through the Use of Fibroreinforced Composites*; Italian Council of Research (CNR): Rome, Italy, 2004.
38. Authority for Electric Energy and Natural Gas, Energy Price. Available online: http://www.autorita.energia.it/it/index.htm (accessed on 5 May 2021). (In Italian)